Caucasian Journal of Science
ISSN: 2148-6840
https://doi.org/10.48138/cjo.1025061
Year: 2021
Volume: 8 Issue: 2

Conformational and Vibrational Analysis of Chalcone (E)-3-(Furan-2-yl)-1-Phenylprop-2-en-1-one by Density Functional Theory and *ab initio* Hartree-Fock

Güventürk UĞURLU[1]

Makalenin Alanı: Fizik

Article Info

Geliş Tarihi
17.11.2021

KabulTarihi
28.12.2021

Anahtar Kelimeler
Titreşim spektrumu
DFT
Öncü moleküler orbital
Patansiyel enerji eğrisi
$C_{13}H_{10}O_2$

ÖZ

Chalcone (E)-3-(Furan-2-yl)-1-Phenylprop-2-en-1-one (1)'in potansiyel enerji eğrileri (PEC), bir fonksiyon dihedral açı ϕ(C8-C9-) olarak hesaplandı. C10-O1), 6-311++G (d,p) temel seti ve düşük karşılık gelen syn- ve anti-uyumlular ile birlikte B3LYP fonksiyonelini kullanan hem başlangıçta Hartree–Fock (HF) hem de Yoğunluk Fonksiyonel Teorisinde (DFT) enerji konformerleri belirlendi. Başlık molekülünün syn- ve anti-conformer'larının optimize edilmiş moleküler yapıları, titreşim dalga sayıları yukarıda bahsedilen iki yöntemle elde edilmiştir. 1H-NMR ve 13C-NMR kimyasal kayma değerleri ve sınır moleküler orbitaller (FMO'lar), her iki konformerin optimize edilmiş yapısından 6-311++G(d,p) temel seti ile DFT/B3LYP ve HF yöntemleri ile hesaplandı. Ayrıca TD-DFT/B3LYP/6-311++G (d,p) hesaplaması ile gaz fazında her iki konformer malın UV-Vis spektrumu hesaplanmıştır. Anti ve syn konformerin denge durumu (temel durum) dipol moment değerleri B3LYP/6-311++ G(d,p) ile 3.33 ve 3.01 Debye ve ab initio HF/6-311 ile 4.05 ve 3.88 Debye olarak hesaplanmıştır. ++ G(d,p) yöntemi. Molekülün hesaplanan geometrik parametreleri (bağ uzunlukları ve bağ-dihedral açıları) literatürdeki deneysel değerlerle karşılaştırılmış ve iyi bir uyum içinde oldukları görülmüştür. Hesaplama dosyasından üretilen çıktı chk.file, elektrostatik potansiyel haritasını ve HOMO-LUMO orbitallerini GaussView5.0.9 programı kullanılarak görselleştirmek için kullanıldı.

Article Info

Received
17.11.2021

Accepted
28.12.2021

Keywords
Vibrational spectra
DFT
frontier molecular orbitals
Potential energy curve
$C_{13}H_{10}O_2$

Abstract

The potential energy curves (PEC) of Chalcone (E)-3-(Furan-2-yl)-1-Phenylprop-2-en-1-one (1) were calculated as a function dihedral angle ϕ(C8-C9-C10-O1) at both *ab initio* Hartree–Fock (HF) and Density Functional Theory (DFT) using the B3LYP functional together with 6-311++G (d,p) basis set and the syn- and anti-conformers corresponding low energy conformers were determined. The optimized molecular structures, vibrational wavenumbers of the syn- and anti-conformers of title molecule were obtained with the two methods mentioned above. The ^{1}H- NMR and ^{13}C-NMR chemical shift values and frontier molecular orbitals (FMOs) were computed from the optimized structure of both conformers by DFT/B3LYP and HF methods with 6-311++G(d,p) basis set. Also, UV-Vis spectrum of both conformers ware calculated in gas phase via TD-DFT/ B3LYP/6-311++G (d,p) calculation. The equilibrium state (ground state) dipole moment values of the anti and syn conformer were calculated as 3.33 and 3.01 Debye by B3LYP/6-311++ G(d,p) and 4.05 and 3.88 Debye by *ab initio* HF/6-311++ G(d,p) method. The calculated geometric parameters (bond lengths and bond-dihedral angles) of the molecule were compared with the experimental values in the literature and they were found to be in good agreement. The output chk.file generated from calculation file was

---

[1] Kafkas University Faculty of Sciences and Letter Department of Physics-Kars; e-mail: gugurlu@kafkas.edu.tr; ORCID: 0000-0003-4171-7879 (Sorumlu yazar)

used to visualize the electrostatic potential map, and HOMO-LUMO orbitals using GaussView5.0.9 program.

Introduction

Chalcones are one of the important compounds with an enormous number of diverse biological activities. They are natural products exist in diverse plant kind such as in vegetables, fruits, tea and soy (Middleton, et al. 2000; Nowakowska, et al. 2007). Synthesis and characterization of new compounds containing chalcone and its derivatives continues increasingly owing to their influence as a drug for variety of promising biological activities such as different anti-diabetic (Hsieh, et al. 2012), anti-cancerous (Saxena, et al. 2007), anti-malarial (Domínguez, et al. 2005), anti-inflammatory (Herencia, et al. 1998), anti-tumour (Kumar, et al. 2003), and tyrosinase inhibitor (Akhtar, et al. 2015), anti-oxidant (Jayasinghe, et al. 2006), analgesic (Tanaka, et al. 2009), antiulcer (Batovska, et al. 2009), antimalarial (Ravichandran, et al. 2015) and antihelmintic(Liu, et al. 2001). Also, they are great intermediates for the synthesis of diverse heterocyclic compounds like isoxazole (Kaur, et al. 2013), pyrazoline (Reddy, et al. 2016), epoxide (Farooq, et al. 2020), thiazine (Badshah, et al.2016), indazole (Shakil, et al. 2013) and pyrimidine valuable in pharmaceutical industries (Bhat, et al. 2017). Crystal structure of molecule (1) were determined experimentally using X-ray structure analysis and spectroscopic methods (Vazquez-Vuelvas et al., 2015) but molecular properties such as electronic energy, conformation and vibration analysis of title molecule have not been determined. In this work, molecular structure, dipole moment, vibrational frequency, the electronic structure and HOMO-LUMO energies of above-mentioned molecule have been studied. The calculated geometric parameters (bond lengths and bond-dihedral angles) of the molecule were compared with the experimental values in the literature and they were found to be in good agreement. ^{1}H NMR and ^{13}C NMR chemical shifts calculations have been performed. Also, the energy band gap of Chalcone (E)-3-(Furan-2-yl)-1-Phenylprop-2-en-1-one molecule is calculated by using the highest occupied molecular orbital (HOMO) energy and the lowest unoccupied molecular orbital (LUMO) energy. The molecular structure using numbering scheme of the compound (1) is given in Figure 1

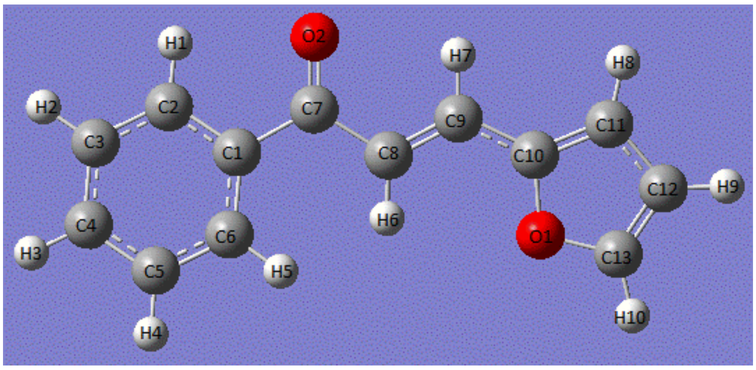

Figure 1. Chalcone (E)-3-(Furan-2-yl)-1-Phenylprop-2-en-1-one molecule numbering scheme

Computational detail

First, the initial geometry of the molecule was modeled in the GaussView 5.0.9 program (Dennington, et al., 2009) and used as input data to determine conformational analysis. The conformational analysis were carried out by calculating the PECs as a function of the torsion angles ϕ(C8-C9-C10-O1) at both ab initio HF and DFT (Kohn et al., 1965) method with standard 6-311++G(d,p) basis set. In the result of conformational analysis, the anti and syn conformers corresponding with low energy on potential energy curves obtained both methods were determined. The molecular geometry of the determined conformers are optimized without any symmetry constraint (preference) at both ab initio HF and DFT method with a hybrid functional B3LYP (Becke's three parameter hybrid functional using the LYP correlation functional) (Becke et al., 1988; Lee et al., 1988; Becke, 1993) in combination with 6-311++G(d,p) basis set. The optimized molecular structures, vibrational wavenumbers of the syn- and anti-conformers of title molecule were obtained with the two methods mentioned above. Also, ^{1}H-NMR and ^{13}C-NMR chemical shift values and frontier molecular orbitals (FMOs) were computed from the optimized structure of both conformers by DFT/B3LYP and HF methods with 6-311++G(d, p) basis set. Also, UV-Vis spectrum of both conformers ware calculated in gas phase via TD-DFT/ B3LYP / 6-311++G (d,p) calculation. The output chk.file generated from calculation file was used to visualize the electrostatic potential map, and HOMO-LUMO orbitals using GaussView5.0.9 program. The quantum mechanics calculations were performed by the aid of Gaussian 09W program package (Frisch et al., 2010) in the gas phase.

RESULTS AND DISCUSSION

Conformational analysis

The conformational analysis were carried out by calculating the PECs as a function of the torsion angles ϕ(C8-C9-C10-O1) at both ab initio HF and DFT method with standard 6-311++G(d,p) basis set. The PECs were calculated by varying dihedral angle ϕ (C9-C10 single bond) from 0° to 180° in 10° increments. In the result of conformational analysis, the anti and syn conformers corresponding with low energy on potential energy curves obtained both methods were determined. The PECs obtained both methods are given Figure 2. As seen from figure 2., the calculated PECs exist two minima, one of these is corresponded syn conformer with ϕ(C8-C9-C10-O1) of 180°. The other conformer, syn conformer with dihedral angle of 180°, exist local minimum, this is 1.27 kcal/mol and 2.35 kcal/mol higher in energy than anti conformer at the DFT/B3LYP and HF methods, respectively. Also, the energy obtained by at the DFT/B3LYP of orthogonal conformation is higher than that of HF method. The difference energy of syn conformer relate to methods, the energy calculated HF method is 1.08 kcal/mol than that of DFT/B3LYP method. In our previous studies (Uğurlu, et al. 2007; 2020), we have not encountered a situation with such a large energy difference.

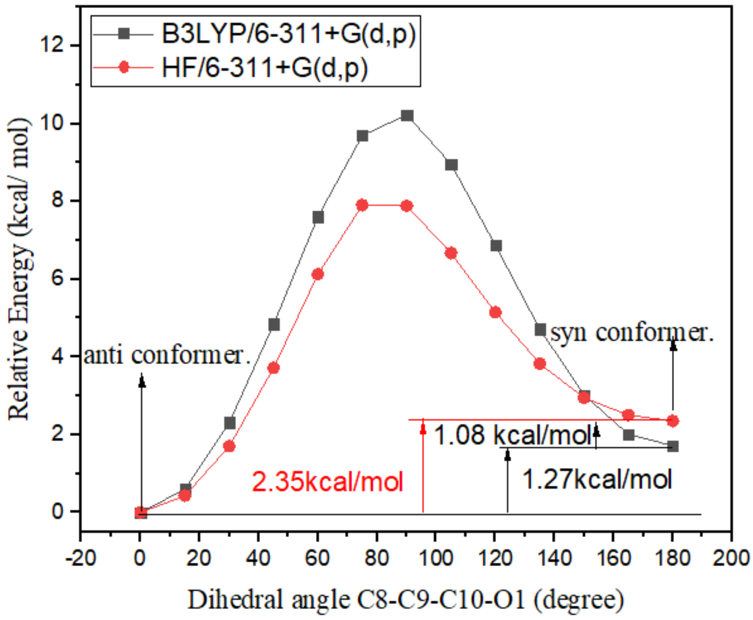

Figure 2. The potential energy curves of Chalcone (E)-3-(Furan-2-yl)-1-Phenylprop-2-en-1-one molecule

Molecular structure

The equilibrium state structures of (1) compound obtained by the HF/6-311++ G (d,p) and DFT/6-311++G (d,p) methods are compiled. The X-ray crystal structures for studied molecule is available in the literature (Vazquez-Vuelvas et al., 2015) and the calculated parameter of studied molecule of both at the B3LYP/6-311++G (d, p) and the HF/6-311++ G (d,p) methods in the ground state are tabulated in the Table 1. As seen from Table 1. in the anti-conformer, the center C9-C10 single bond length of dihedral angle ϕ(C8-C9-C10-O1) is 1.4305Å at the B3LYP/6-311++G (d, p) and 1.4480 Å at HF/6-311++ G (d,p), In the syn-conformer, 1.3643Å at the B3LYP/6-311++G (d, p) and 1.3443Å at HF/6-311++ G (d,p), respectively. This observed value is 1.4236 Å**.** For C9-C10 single bond, the calculated bond lengths in the anti-conformer both methods are larger than the bond lengths in the syn conformer and are closer to the experimental value. Also, regression analyses of the bond length values in the Table 1 were carried out and in the results of regression analyses, it has been shown that there is a linear correlation between experimental and theoretical bond lengths. It was observed that the calculated optimal R^2 value was 0.9811 at anti-conformer with B3LYP/6-311++G (d,p). In the anti-conformer, dihedral angle ϕ(C8-C9-C10-O1) is 0.02° at the B3LYP/6-311++G (d, p) and 0.05° at HF/6-311++ G (d,p), in the syn-conformer, -179.18° at the B3LYP/6-311++G (d, p) and -178.90° at HF/6-311++ G (d,p), respectively. The experimental value of this dihedral angle was observed as -3.20° (Vazquez-Vuelvas et al., 2015). In the both methods and both conformer, dihedral angle ϕ(C8-C9-C10-O1) is planer almost.

Table 1. Selected structural parameters of Chalcone (E)-3-(Furan-2-yl)-1-Phenylprop-2-en-1-one molecule

Bond length (Å)	anti-conformer			syn-conformer	
Atoms	DFT	HF	Exp[a].	DFT	HF
O1—C13	1.3568	1.3389	1.3627 (17)	1.3525	1.3352
O1—C10	1.3739	1.3470	1.3628(15)	1.3765	1.3847
C1—C7	1.5032	1.5019	1.4882 (17)	1.5030	1.5802
O2—C7	1.2256	1.1952	1.2218 (15)	1.2248	1.1944
C7—C8	1.4801	1.4896	1.4664 (18)	1.4803	1.4897
C9—C8	1.3485	1.3278	1.3308 (17)	1.3484	1.3276
C9—C10	1.4305	1.4480	1.4236 (18)	1.4335	1.4534
C12—C13	1.3625	1.3410	1.327 (2)	1.3643	1.3423
R^2	0.9811	0.9794		0.9767	0.9594
Bond angle (˚)					
C2-C1-C7	118.77	117.86	118.43 (11)	117.78	117.90
C6-C1-C7	123.55	123.05	122.76 (12)	123.40	122.98
O2-C7-C8	121.14	121.07	120.74 (12)	121.31	121.18

O2-C7-C1	119.87	120.07	119.78 (12)	119.92	120.10
C8-C7-C1	118.98	118.86	119.44 (11)	118.76	118.70
C8-C9-C10	126.31	125.33	127.34(12)	126.21	125.64
C9-C8-C7	120.16	119.96	121.16 (12)	120.34	120.10
O1-C10-C9	119.35	119.22	118.76 (11)	115.97	115.76
Dihedral angle (˚)					
C2-C1-C7-O2	10.01	15.93	19.4 (2)	14.32	18.38
C6-C1-C7-O2	-169.05	-162.72	-159.66 (14)	-164.25	-160.14
C2-C1-C7-C8	-169.00	-163.40	-158.15 (13)	-164.90	-160.81
C6-C1-C7-C8	11.00	17.95	22.74 (19)	16.53	20.67
C10-C9-C8-C7	-179.21	-179.30	-176.31 (13)	-178.98	-178.90
O2-C7-C8-C9	2.77	8.09	-5.4 (2)	4.63	9.12
C1-C7-C8-C9	-177.84	-172.59	172.14 (12)	-176.18	-171.70
C8-C9-C10-O1	0.02	0.05	-3.2 (2)	-179.08	-177.21
C7-C1-C2-C3	-179.59	-179.39	-179.11 (14)	-179.29	-179.35
C2-C1-C6-C5	0.03	0.00	-0.7 (2)	0.00	0.00
C7-C1-C6-C5	179.07	178.63	178.37 (13)	178.55	178.51
C1-C6-C5-C4	0.43	0.06	0.80 (2)	0.60	0.69
C8-C9-C10-C11	179.96	179.95	173.72 (14)	0.99	3.09

(([a]) ref Vazquez-Vuelvas et al., 2015)

The surface of the highest occupied molecular orbital (HOMO) energy, the lowest unoccupied molecular orbital (LUMO) energy and the electrostatic potential map are given Figure 3 and 4., respectively.

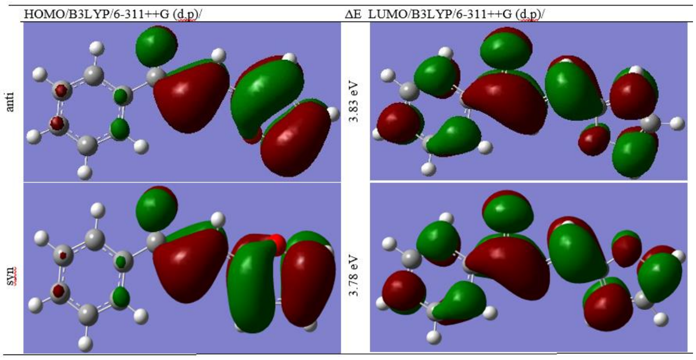

Figure 3. The surface of HOMO-LUMO orbitals of Chalcone (E)-3-(Furan-2-yl)-1-Phenylprop-2-en-1-one

The anti-conformer of (1) molecule the transitions are calculated at wavelengths 384.65, 339.28 and 299.83 nm and for syn conformer at 385.80, 344.94 and 299.44 nm in the gas phase at the B3LYP/6-311++G(d,p) level of theory.

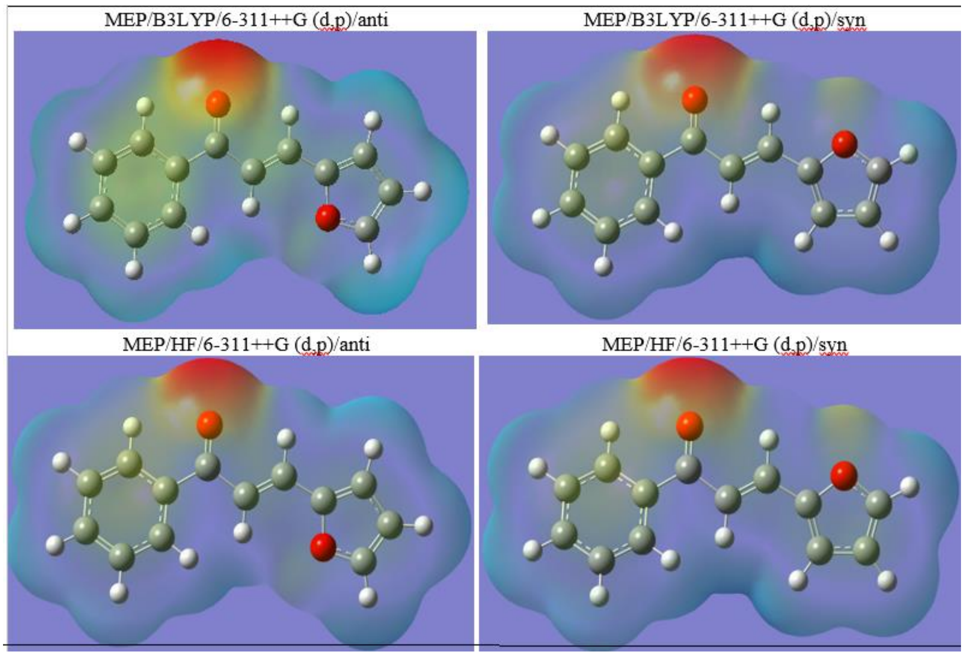

Figure 4. the electrostatic potential map of Chalcone (E)-3-(Furan-2-yl)-1-Phenylprop-2-en-1-one

Vibrational Frequencies

Chalcone (E)-3-(Furan-2-yl)-1-Phenylprop-2-en-1-one molecule consist of 25 atoms having 69 normal modes of vibrations. The vibrational frequency values calculated B3LYP/6-311++G(d,p) level were scaled with 0.958 for ($\upsilon > 1700$ cm $^{-1}$) , 0983 for ($\upsilon < 1700$ cm $^{-1}$) (Çelik, et al., 2021) and HF/6-311++G(d,p) level were scaled with 0.9607 (Govindarajan, et al.,2018; Uğurlu, et al. 2018; 2020). Also, the calculated vibrational assignments of the normal modes were performed on the basis of the Potential Energy Distribution (PED) and it has been calculated using the Vibrational Energy Distribution Analysis VEDA 4 program (Jomroz, 2004). The calculated IR and Raman spectrum of (1) molecule are given Figure 5 and 6., respectively.

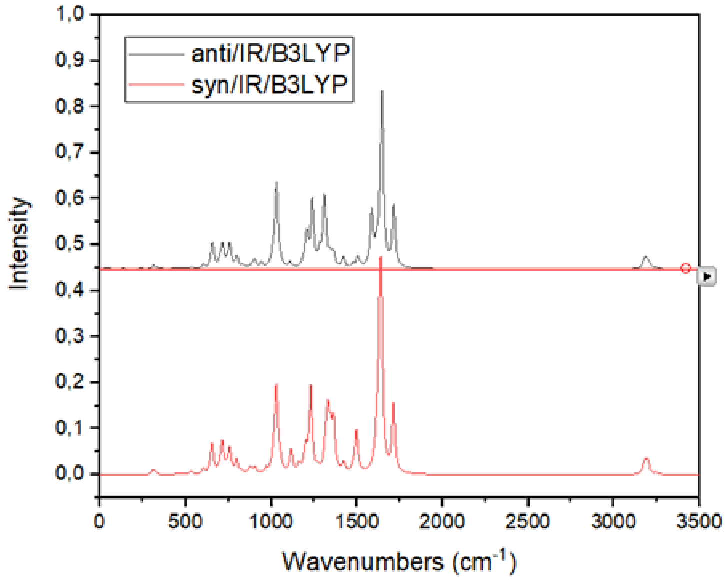

Figure 5. calculated IR spectrum of (1) molecule with 6-311++ G (d,p).

In the both methods and both conformer, the calculated vibrational frequencies of (1) molecule are given Table 2 and 3., respectively.

Table 2. the vibrational frequencies of of (1) molecule with 6-311++ G (d,p)

anti	Theoretical wavenumbers (cm^{-1}) *(Unscaled abbreviated as Unsc)*				
	DFT		HF		*(Scaled abbreviated as Sc)*
Exp.	*Unsc.*	*Sc.*	*Unsc.*	*Sc*	Assignments with PED (≥10 %)
3123	3277	3140	3436	3116	vC11H(11) vC13H(81)
3123	3255	3118	3408	3090	vC11H(85) vC13H(13)
	3244	3108	3396	3080	vC12H(91)
	3215	3080	3384	3068	vC6H(39) vC8H(12) vC9H(46)
	3201	3067	3371	3057	vC2H(27) vC4H(11) vC5H(53)
	3195	3061	3359	3046	vC2H(13) vC8H(62)
3035	3185	3051	3350	3038	vC2H(15) vC3H(29) vC5H(35) vC8H(13)
	3174	3041	3346	3034	v C2H(36) vC3H(53)
	3168	3035	3335	3023	v C6H(47) vC9H(47)
	3164	3031	3321	3011	v C4H(81)
1658	1714	1685	1923	1743	v O2C7(54) vC11C10(11)
	1646	1618	1832	1661	vO2C7(17) vC9C8(10) vC12C13(16) vC10C9(10)
1594	1635	1607	1786	1620	vC11C10(21) vC4C3(14)
	1614	1586	1760	1596	vC4C3(40)
1545	1586	1559	1745	1582	v C2C3(51) βHC11C12(11)
	1521	1495	1655	1501	vC1C6(13) βHC2C3(38)
1474	1504	1479	1647	1493	vC9C8(33) vC12C13(20) βHC13O1(17)
	1475	1450	1592	1443	vC1C6(16) βHC3C4(10) βHC6C5(33)
	1420	1396	1545	1401	βHC11C12(20) βHC13O1(12) βC12C13O1(35)
	1364	1340	1471	1334	βHC6C5(29) βHC6C5(24) βHC9C10(14)
	1345	1322	1438	1304	vC5C4(48) βHC8C9(12)
	1322	1300	1416	1284	vC5C4(11) βHC6C5(17) βHC8C9(27)

1310	1288	1386	1256	νC8C7(10)HC6C5(17)
1281	1260	1339	1214	νO1C13 (14) βHC9C10(24)
1239	1218	1329	1205	C7C1(20) βHC11C12(20) βHC13O1(10)
1210	1189	1311	1189	ν C7C1(10) βHC9C10(35)
1201	1181	1288	1168	βHC3C4(42) βHC8C9(12)
1183	1163	1274	1155	νC5C4(11) βHC4C5(71)
1176	1156	1215	1101	νO1C10 (40) βHC11C12(10) βHC13O1(29)
1109	1091	1195	1084	νO1C13 (10)
1105	1086	1172	1063	O1C13 (14) βHC11C12(12)
1053	1035	1125	1020	νC1C6(10) νC6C5(11) βHC2C3(11) βC9C8C7(19)
1040	1023	1120	1015	γHC11C12(52) βC12C13O1(13) βO1C10C9(11)
1030	1012	1113	1009	νC6C5(10) νC8C7(14) νC10C9(16) βC10C9C8(15)
1016	999	1108	1004	νC6C5(28) βC6C5C4(32) βC9C8C7(16)
1011	994	1100	997	γHC4C5C6(39) γHC6C5C4(13) γHC8C9C10(16)
1008	991	1092	990	γHC4C5C6(28) γHC6C5C4(20) γHC8C9C10(20)
990	974	1081	980	γHC3C4C5(56)
947	931	1058	959	γHC2C3C4(40) γHC6C5C4(20)
942	926	1031	935	νO1C10 (23) ν O1C13 (20) βC12C13O1(10)
902	887	1010	916	νO1C10 (13) βC11C10O1(57) βC12C13O1(10)
895	880	995	902	γHC9C10C11(25) γHC12C13O1(40)
888	873	971	881	γHC8C9C10(13) γHC9C10C11(26) γHC12C13O1(34)
877	862	950	862	βO2C7C8(15) βC5C4C3(14) βC9C8C7(10)
857	843	945	857	γHC2C3C4(45) γHC3C4C5(10) γHC5C6C1(12)
831	817	944	856	γHC11C12C13(69)
798	784	875	793	γHC5C6C1(23) γHC9C10C11(14) γHC11C12C13(10)
757	744	856	776	γHC13O1C10(87)
740	727	791	717	νC8C7(19) νC7C1(12) βC11C10O1(11) βO1C10C9(10)
714	702	783	710	γHC5C6C1(34) γO2C1C8C7(24) γC11C9O1C10(12)
699	687	756	685	γHC4C5C6(11) γHC5C6C1(15) γC1C6C5C4(26)
658	646	714	648	βO2C7C8(12) γO2C1C8C7(10) γC11C9O1C10(24)
654	642	697	632	βO2C7C8(20) γC11C9O1C10(16)
632	621	673	610	βC2C3C4(33) γC5C4C3(32)
603	593	650	590	γHC12C13O1(16) γC2C3C4C5(12) γC6C5C4C3(15)
532	523	568	515	βC1C6C5(12) γC13O1C10(16) γC7C1C6(36)
454	447	495	448	γC6C5C4C3(18) γC9C8C7C1(14) γC7C2C6C1(19)
428	420	451	409	νC7C1(15) βO2C7C8(10) βC7C1C6(15)
410	403	450	408	γHC3C4C5(15) γC2C3C4C5(31) γC12C12O1C10(24)
338	332	359	326	γC10C9C8C7(10) γO1C10C9C8(50) γC11C9O1C10(13)
312	307	329	298	βO2C7C8(18) βC6C5C4(12) βC13O1C10(10)
237	233	252	229	ν C10C9(24) ν C7C1(12) βC2C3C4(10) βC8C7C1(15)
207	204	229	207	βC8C7C1(12) γC2C3C4C5(12) γC9C8C7C1(15)
173	170	173	157	βC8C7C1(24) γC9C8C7C1(11)
133	131	140	127	γC2C3C4C5(11) γC6C5C4C3(11) γC13O1C10C9(21)
98	97	108	98	γC1C6C5C4(23) γC10C9C8C7(20) γO1C10C9C8(14)
60	59	63	57	βC1C6C5(21) βC13O1C10(10) βC8C7C1(27)
36	36	34	31	γC6C5C4C3(22) γC12C12O1C10(28) γC13O1C10C9(13)
19	19	32	29	γC8C7C1C2(82)

(ν: stretching, β: in- plane bending, γ: out-of-plane bending)

Table 3. the vibrational frequencies of (1) molecule with 6-311++ G (d,p)

syn			Theoretical wavenumbers (cm^{-1}) (*Unscaled abbreviated as Unsc)*		
	DFT		HF		*(Scaled* abbreviated as *S*c)
Exp.	*Unsc.*	*Sc.*	*Unsc.*	*Sc.*	Assignments with PED (≥10 %)
3123	3277	3140	3437	3116	νC11H(11) νC13H(81)
3123	3255	3119	3409	3091	νC11H(85) νC13H(13)
	3244	3108	3397	3080	νC12H(91)
	3201	3067	3370	3056	νC6H(39) νC8H(12) νC9H(46)
	3200	3065	3368	3054	νC2H(27) νC4H(11) νC5H(53)
	3188	3055	3353	3040	νC2H(13) νC8H(62)
3035	3183	3049	3350	3037	νC2H(15) νC3H(29) νC5H(35) νC8H(13)
	3174	3040	3345	3033	νC2H(36) νC3H(53)
	3166	3033	3334	3023	νC6H(47) νC9H(47)
	3164	3031	3321	3011	νC4H(81)
1658	1713	1641	1925	1746	νO2C7(54) νC11C10(11)
	1641	1573	1821	1651	νO2C7(17) νC9C8(10) νC12C13(16) νC10C9(10)
1594	1632	1564	1786	1620	νC11C10(21) νC4C3(14)
	1614	1546	1763	1598	νC4C3(40)
1545	1599	1532	1760	1596	νC2C3(51) βHC11C12(11)
	1521	1457	1649	1495	νC1C6(13) βHC2C3(38)
1474	1497	1434	1647	1493	νC9C8(33) νC12C13(20) βHC13O1(17)
	1476	1414	1592	1443	νC1C6(16) βHC3C4(10) βHC6C5(33)
	1423	1363	1542	1398	βHC11C12(20) βHC13O1(12) βC12C13O1(35)
	1364	1307	1471	1334	βHC6C5(29) βHC6C5(24) βHC9C10(14)
	1346	1290	1442	1307	νC5C4(48) βHC8C9(12)
	1330	1274	1429	1296	νC5C4(11) βHC6C5(17) βHC8C9(27)
	1317	1261	1366	1238	νC8C7(10)HC6C5(17)
	1271	1217	1338	1213	νO1C13 (14) βHC9C10(24)
	1230	1178	1325	1201	νC7C1(20) βHC11C12(20) βHC13O1(10)
	1202	1151	1307	1185	νC7C1(10) βHC9C10(35)
	1192	1142	1288	1168	βHC3C4(42) βHC8C9(12)
	1183	1133	1252	1135	βC5C4(11) βHC4C5(71)
	1161	1112	1214	1101	νO1C10 (40) βHC11C12(10) βHC13O1(29)
	1116	1069	1200	1088	νO1C13 (10)
	1107	1060	1172	1062	νO1C13 (14) βHC11C12(12)
	1053	1009	1125	1020	νC1C6(10) νC6C5(11) βHC2C3(11) βC9C8C7(19)
	1042	999	1121	1016	βHC11C12(52) βC12C13O1(13) βO1C10C9(11)
	1028	985	1117	1013	νC6C5(10) νC8C7(14) νC10C9(16) βC10C9C8(15)
	1017	974	1108	1004	νC6C5(28) βC6C5C4(32) βC9C8C7(16)
	1012	969	1100	997	γHC4C5C6(39) γHC6C5C4(13) γHC8C9C10(16)
	1008	966	1095	993	γHC4C5C6(28) γHC6C5C4(20) γHC8C9C10(20)
	990	948	1081	980	γHC3C4C5(56)
	969	929	1058	959	γHC2C3C4(40) γHC6C5C4(20)
	946	907	1054	956	νO1C10 (23) νO1C13 (20) βC12C13O1(10)
	904	866	1009	915	νO1C10 (13) βC11C10O1(57) βC12C13O1(10)
	889	852	986	894	γHC9C10C11(25) γHC12C13O1(40)
	881	844	973	882	βHC8C9C10(13) βHC9C10C11(26) βHC12C13O1(34)
	871	835	951	862	βO2C7C8(15) βC5C4C3(14) βC9C8C7(10)

857	821	942	854	γHC2C3C4(45) γβHC3C4C5(10) γHC5C6C1(12) γHC6C5C4(14)
826	792	940	852	γHC11C12C13(69)
796	763	874	792	γHC5C6C1(23) γHC9C10C11(14) γHC11C12C13(10)
756	724	856	776	γHC13O1C10(87)
739	708	791	717	C8C7(19)C7C1(12)C11C10O1(11)O1C10C9(10)
712	682	781	708	γHC5C6C1(34) γO2C1C8C7(24) γC11C9O1C10(12)
699	669	756	686	γHC4C5C6(11) γHC5C6C1(15) γC1C6C5C4(26) γC10C9C8C7(15)
654	626	706	641	βO2C7C8(12) γO2C1C8C7(10) γC11C9O1C10(24)
645	618	693	629	βO2C7C8(20) γC11C9O1C10(16)
632	605	673	610	βC2C3C4(33) βC5C4C3(32)
602	576	649	589	γHC12C13O1(16) γβC2C3C4C5(12) γC6C5C4C3(15)
530	508	565	513	βC1C6C5(12) βC13O1C10(16) βC7C1C6(36)
455	436	493	447	γC6C5C4C3(18) γC9C8C7C1(14) γC7C2C6C1(19)
421	403	451	409	vC7C1(15) βO2C7C8(10) βC7C1C6(15)
411	394	446	404	γHC3C4C5(15) γC2C3C4C5(31) γC12C12O1C10(24)
321	307	345	313	γC10C9C8C7(10) γO1C10C9C8(50) γC11C9O1C10(13)
309	296	327	296	βO2C7C8(18) βC6C5C4(12) βC13O1C10(10) βC7C1C6(17)
231	221	244	221	βC10C9(24) βC7C1(12) βC2C3C4(10) βC8C7C1(15)
211	202	227	206	βC8C7C1(12) γC2C3C4C5(12) γC9C8C7C1(15)
163	156	170	154	βC8C7C1(24) γC9C8C7C1(11)
122	117	115	104	γC2C3C4C5(11) γC6C5C4C3(11) γC13O1C10C9(21)
97	93	101	91	γC1C6C5C4(23) γC10C9C8C7(20) γO1C10C9C8(14)
62	59	63	57	βC1C6C5(21) βC13O1C10(10) βC8C7C1(27)
33	31	35	32	γC6C5C4C3(22) γC12C12O1C10(41)
28	27	23	21	γC8C7C1C2(82)

(([a]) ref Vazquez-Vuelvas et al., 2015)

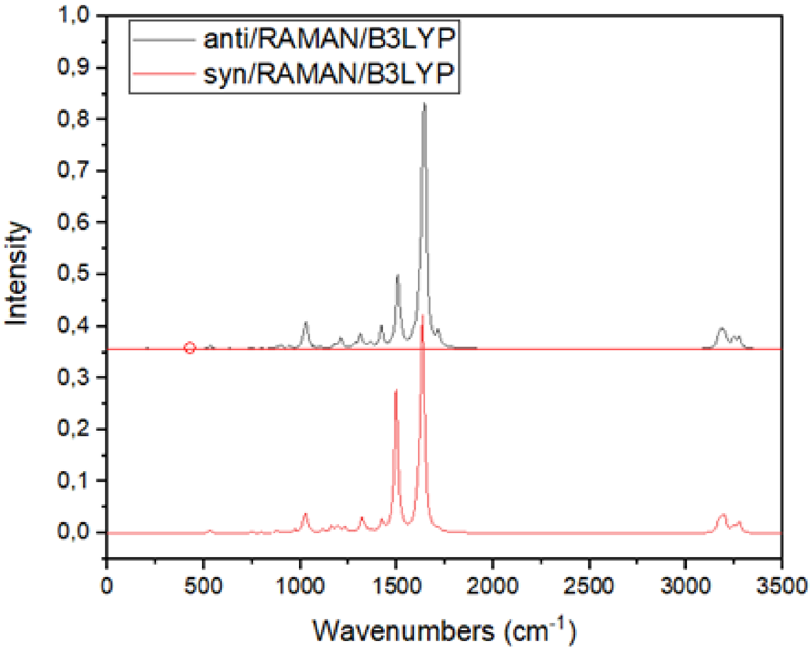

Figure 6. The calculated Raman spectrum of (1) molecule with 6-311++ G (d,p)

The geometry of the studied molecule belongs to C_1 point group symmetry and as seen figure 3 and 4, all vibrations are active in both IR and Raman.

^{1}H and ^{13}C NMR Chemical Shift

Table 4. The calculated chemical shifts (ppm) of (1) molecule with B3LYP

anti-		6-31G		6-31G+(d)		6-31G+(d,p)		6-31G++(d)		6-31G++(d,p)	
No	Exp[a].	GAS	DMSO	GAS	DMSO	GAS	DMSO	GAS	DMSO	GAS	DMSO
C7	189.95	181.48	183.24	178.64	181.17	180.34	182.71	189.47	201.18	171.43	182.92
C10	151.69	150.29	149.37	149.66	148.94	151.63	150.48	160.27	168.19	142.49	150.67
C13	144.98	140.91	143.81	139.50	143.16	140.52	144.70	149.99	162.54	131.28	143.94
C1	138.16	135.05	135.03	134.50	134.65	136.47	136.19	145.24	152.39	127.43	136.53
C4	132.82	127.43	129.44	126.74	129.32	127.79	130.86	137.26	147.84	118.58	130.14
C9	130.72	125.79	127.58	126.00	127.97	127.32	129.51	136.64	145.56	118.13	129.06
C2	128.47	125.67	125.19	125.92	125.26	126.97	126.79	136.53	143.00	117.93	126.17
C6	128.47	124.42	125.18	123.71	125.23	124.80	126.77	134.40	142.59	115.77	126.03
C3	128.47	123.55	124.91	123.21	124.90	124.14	126.44	133.76	142.54	115.01	125.93
C5	128.47	123.27	124.80	122.57	124.70	123.66	126.24	133.00	142.27	114.40	125.51
C8	119.30	115.41	118.99	113.78	118.01	114.64	119.55	124.35	135.84	105.76	118.87
C11	116.33	115.34	115.02	113.27	113.09	114.46	114.63	124.30	127.83	105.60	114.51
C12	112.74	111.08	112.67	108.01	109.91	109.09	111.45	118.54	127.57	99.95	110.86
R^2		0.9915	0.9958	0.9906	0.9962	0.9886	0.9962	0.9903	0.9919	0.9886	0.9962
H1	8.04	8.51	8.36	8.45	8.33	8.70	7.87	9.12	8.39	8.96	8.61
H7	8.04	7.89	7.92	7.69	7.75	7.99	7.30	8.36	7.83	8.25	8.08
H6	7.61	7.85	7.91	7.37	7.48	7.76	7.02	8.02	7.57	8.01	7.88
H10	7.58	7.82	8.06	7.96	8.22	8.19	7.76	8.65	8.27	8.48	8.49
H5	7.52	7.57	7.84	7.46	7.75	7.73	7.29	8.14	7.79	8.01	8.05
H2	7.52	7.51	7.69	7.45	7.62	7.62	7.17	8.12	7.70	7.90	7.84
H3	7.49	7.45	7.72	7.51	7.78	7.65	7.32	8.18	7.81	7.92	7.95
H4	7.47	7.44	7.69	7.43	7.68	7.60	7.23	8.12	7.72	7.90	7.91
H8	6.72	6.65	7.00	6.56	6.92	6.83	6.46	7.23	6.97	7.13	7.25
H9	6.51	6.51	6.79	6.41	6.66	6.70	6.21	7.07	6.61	6.99	7.01

((a) ref Vazquez-Vuelvas et al., 2015)

The ^{1}H NMR and ^{13}C NMR chemical shifts of Chalcone (E)-3-(Furan-2-Yl)-1-Phenylprop-2-en-1-one molecule are calculated using the gauge-independent atomic orbital method (GIAO method) and the hybrid three-parameter B3LYP density functional in combination and Hartree-fock methods with different basis sets such as 6-31G, 6-31+G(d), 6-31+G(d.p), 6-31++G(d), and 6-31++G(d.p) basis sets in gas phase and in solvents (DMSO).

The calculated ^{1}H and ^{13}C chemical shielding values calculated B3LYP/6-31G, B3LYP/6-31+G(d), B3LYP/6-31+G(d.p), B3LYP/6-31++G(d), and B3LYP/6-31++G(d.p) are given in the Table 4. The calculated ^{1}H and ^{13}C chemical shielding values calculated HF/6-31G, HF/6-

31+G(d), HF/6-31+G(d.p), HF/6-31++G(d), and HF/6-31++G(d.p) are given in the Table 5. Also, the value ^{13}C NMR chemical shifts are carried regression analyses and the results were indicated linear correlation.

Table 5. The calculated chemical shifts (ppm) of (1) molecule with HF

anti-		6-31G		6-31G+(d)(3)		6-31G+(d,p)(4)		6-31G++(d)		6-31G++(d,p)	
No	Exp[a]	GAS	DMSO	GAS	DMSO	GAS	DMSO	GAS	DMSO	GAS	DMSO
C7	189.95	200,29	202,85	187,68	190,71	189,05	192,45	187,96	191,29	189,40	192,72
C10	151.69	158,95	156,86	151,60	149,42	153,30	151,47	151,81	149,92	153,59	151,89
C13	144.98	154,56	157,47	147,29	150,43	148,06	151,55	147,61	151,08	148,45	151,66
C1	138.16	142,40	141,92	137,55	135,99	138,62	138,04	137,82	136,54	138,96	141,74
C4	132.82	141,10	142,37	136,78	137,22	138,47	138,53	137,01	137,80	138,75	138,78
C9	130.72	140,00	144,14	134,82	140,06	135,78	141,49	135,07	140,62	136,10	138,26
C2	128.47	138,62	137,93	134,73	133,72	135,58	134,93	135,03	134,33	135,91	135,20
C6	128.47	135,17	137,17	130,96	132,92	131,79	134,11	131,27	133,53	132,19	134,42
C3	128.47	132,89	133,41	127,25	127,69	128,25	129,05	127,54	128,30	128,62	129,35
C5	128.47	131,60	133,14	125,82	127,37	126,81	128,70	126,11	127,98	127,18	129,02
C8	119.30	124,61	121,30	118,64	112,77	119,27	114,09	118,92	123,82	119,67	124,56
C11	116.33	122,96	129,46	114,53	123,23	115,50	124,23	114,70	113,23	115,71	114,23
C12	112.74	118,10	119,18	109,72	110,36	110,70	111,69	110,02	111,00	111,09	112,03
R^2		0.9902	0.9686	0.9774	0.9478	0.9776	0.9517	0.9774	0.9600	0.9777	0.9747
H1	8.04	9,70	9,55	9,39	9,34	9,47	9,36	9,40	9,29	9,49	9,38
H7	8.04	9,18	9,27	8,78	8,97	8,86	8,97	8,79	8,90	8,87	8,98
H6	7.61	8,54	8,57	7,81	7,98	8,00	8,10	7,80	7,90	7,99	8,09
H5	7.58	8,72	9,04	8,61	9,00	8,70	9,01	8,63	8,95	8,71	9,03
H10	7.52	8,55	8,86	8,12	8,50	8,19	8,49	8,11	8,43	8,20	8,50
H2	7.52	8,25	8,47	7,99	8,26	8,04	8,25	8,01	8,22	8,07	8,28
H3	7.49	8,38	8,73	8,18	8,58	8,21	8,54	8,19	8,53	8,23	8,56
H4	7.47	8,17	8,48	7,93	8,30	7,98	8,28	7,94	8,25	8,00	8,30
H8	6.72	7,49	7,96	7,11	7,63	7,27	7,71	7,12	7,57	7,29	7,73
H9	6.51	7,22	7,54	6,76	7,10	6,96	7,23	6,78	7,05	6,98	7,25

(([a]) ref Vazquez-Vuelvas et al., 2015)

The ^{13}C NMR chemical shifts calculated B3LYP, R^2 6-31G, 6-31+G(d), 6-31+G(d.p), 6-31++G(d), and 6-31++G(d.p), 6-31+G(d) have been 0.9915 ppm, 0.9906 ppm, 0.9886 ppm, 0.9903 ppm, 0,9886 ppm (gas phase) and 0.9958 ppm, 0.9962 ppm, 0.9962 ppm, 0.9919 ppm, 0.9962 ppm DMSO) for 13C-NMR chemical shifts values. The ^{13}C NMR chemical shifts calculated HF, R^2 6-31G, 6-31+G(d), 6-31+G(d.p), 6-31++G(d), and 6-31++G(d.p), 6-31+G(d), have been 0.9902ppm, 0.9774 ppm, 0.9776 ppm, 0.9774 ppm, 0,9777 ppm (gas phase) and 0.9686 ppm, 0.9478 ppm, 0.9517 ppm, 0.9600 ppm, 0.9747 ppm DMSO) for 13C-NMR chemical shifts values. In the ^{13}C NMR chemical shifts calculated B3LYP, R^2 vales in the DMSO are larger than that of in the gas phase and in the 13C NMR chemical shifts calculated B3LYP, R2 vales in gas phase are larger than that of in the DMSO. These results show that there is a good agreement between the experimental values and the theoretical values.

Conclusion

The potential energy curves of (1) molecule were calculated as a function dihedral angle ϕ(C8-C9-C10-O1) at both ab initio HF) and DFT/ B3LYP with 6-311++G (d,p) basis set and the syn- and anti-conformers corresponding low energy conformers were determined. The optimized molecular structures, vibrational wavenumbers of the syn- and anti-conformers of title molecule were obtained with the two methods mentioned above. The 1H- NMR and 13C-NMR chemical shift values and frontier molecular orbitals (FMOs) were computed from the optimized structure of both conformers by DFT/B3LYP and HF methods with 6-311++G(d,p) basis set. The anti-conformer of (1) molecule the transitions are calculated at wavelengths 384.65, 339.28 and 299.83 nm and for syn conformer at 385.80, 344.94 and 299.44 nm in the gas phase atB3LYP/6-311++G(d,p) level of theory. The equilibrium state (ground state) dipole moment values of the anti and syn conformer were calculated as 3.33 and 3.01 Debye by B3LYP/6-311++ G(d,p) and 4.05 and 3.88 Debye by ab initio HF/6-311++ G(d,p) method. In the the both methods and both conformer, dihedral angle ϕ(C8-C9-C10-O1) is planer almost.

REFERENCES

Akhtar, M.N., Sakeh, N.M., Zareen, S., Gul, S., Lo, K.M., Ul-Haq, Z., Shah, S.A.A., Ahmad, S. (2015). Design and synthesis of chalcone derivatives as potent tyrosinase inhibitors and their structural activity relationship, *J. Mol. Struct*. 1085 97–103.

Badshah, S., Naeem, A. (2016) Bioactive Thiazine and Benzothiazine Derivatives: Green Synthesis Methods and Their Medicinal Importance. *Molecules*. 21, 1054.

Batovska, D., Parushev, S., Stamboliyska, B., Tsvetkova, I., Ninova, M., Najdenski, H. (2009). Examination of growth inhibitory properties of synthetic chalcones for which antibacterial activity was predicted. *Eur J Med Chem.* 44: 2211-2218, 2009.

Becke, A. D. (1988) Density-functional exchange-energy approximation with correct asymptotic behavior. *Physical Review A*, 38(6), 3098–3100.

Becke, A. D., 1993. Density-Functional Thermochemistry .3. The Role of Exact Exchange. *J. Chem. Phys.,* 98 (7): 5648-5652.

Bhat, M. A., Khan, A. A., Al-Omar, M. A., Khan, A. A. (2017), “Synthesis and anti-candidal activity of some new pyrazoline derivatives,” *Biomedical Research*, vol. 28, pp. 3082–3087.

Çelik, F., Ustabas¸ R., Süleymanoglu,N., Direkel, S., Güler, H. I., Ünver, Y. (2021). 2,3-triazole derivative: Synthesis, characterization, DFT, molecular docking study and antibacterial-antileishmanial activities Journal of the *Indian Chemical Society*. 98.

Dennington, R., Keith T., Millam, J. (2009). *Semichem Inc., GaussView, Version 5*, Shawnee Mission KS,

Domínguez, J.N., León, C., Rodrigues, J., Domínguez, N.G.D., Gut, J., Rosenthal, P.J. (2005). Synthesis and antimalarial activity of sulfonamide chalcone derivatives, *Il Farmaco*. 60 (4), 307–311.

Farooq, S., Ngaini, Z., Mortadza N. A. (2020) Microwave-assisted Synthesis and Molecular Docking Study of Heteroaromatic Chalcone Derivatives as Potential Antibacterial Agents. *Bull. Korean Chem. Soc*. Vol. 41, 918–924.

Frisch M J, Trucks G W, Schlegel H B, Scuseria G E, Robb M A, Cheeseman J R, Scalmani G, Barone V, Mennucci B, Petersson G A, Nakatsuji H, Caricato M, Li X, Hratchian H P, Izmaylov A F, Bloino J, Zheng G, Sonnenberg J L, Hada M, Ehara M, Toyota K, Fukuda R, Hasegawa J, Ishida,M, Nakajima T, Honda Y, Kitao O, Nakai H, Vreven T, Montgomery J A, Vreven T J, Peralta J E, Ogliaro F, Bearpark M, Heyd J. J, Brothers E, Kudin N, Staroverov V N, Kobayashi R, Normand J, Raghavachari K, Rendell A, Burant J C, Iyengar S S, Tomasi J, Cossi M, Rega N, Millam J M, Klene,M, Knox J E, Cross J B, Bakken V, Adamo C, Jaramillo J, Gomperts R, Stratmann R E, Yazyev O, Austin A J, Cammi R, Pomelli C J, Ochterski W, Martin L R, Morokuma K, Zakrzewski V G, Voth G A, Salvador P, Dannenberg J J, Dapprich S, Daniels A D, Farkas O, Foresman J B, Ortiz J V, Cioslowski J, Fox D J, 2009. *Gaussian Inc.,* (Wallingford, CT).

Govindarajan, M., Salgado-Morán, G., Montes Romero, P., Gerli Candi, L. 2018). A theoretical quantum study of the electronic properties of mentoxy dichloro phosphorous. *J. Chil. Chem. Soc*. Vol.63, 3887-3897.

Herencia, F., Ferrandiz, M.L., Ubeda, A., Domínguez, J.N., Charris, J.E., Lobo, G.M., Alcaraz, M.J. (1998). Synthesis and anti-inflammatory activity of chalcone derivatives, *Bioorg. Med. Chem. Lett*. 8 (10), 1169–1174.

Hsieh, C.T., Hsieh, T. J., El-Shazly, M., Chuang, D.W., Tsai, Y. H., Yen, C.T., Wu, S. F., Wu, Y. C., Chang, F. R. (2012). Synthesis of chalcone derivatives as poten tial anti-diabetic agents, *Bioorg. Med. chem. Lett*. 22 (12), 3912–3915.

Jamroz, M. H. (2004). *Vibrational Energy Distribution Analysis VEDA Computer program*. Poland

Jayasinghe, L., Rupasinghe, G.K., Hara, N., Fujimoto, Y. (2006) Geranylated phenolic constituents from the fruits of Artocarpus nobilis. *Phytochemistry.* 67: 1353-1358.

Kaur, N., Kishore, D. (2013). Application of chalcones in heterocycles synthesis:Synthesis of 2-(isoxazolo, pyrazolo and pyrimido) substitutedanalogues of 1,4-benzodiazepin-5-carboxamides linkedthrough an oxyphenyl bridge. *J. Chem. Sci.* 125, 555.

Kohn, W., Sham, L.J.(1965) Self-Consistent Equations Including Exchange and Correlation Effects, *Phys. Rev.* 140 A1133–A1138.

Kumar, S.K., Hager, E., Pettit, C., Gurulingappa, H., Davidson, N.E., Khan, S.R., (2003). Design, synthesis, and evaluation of novel boronic-chalcone derivatives as antitu-mor agents, *J. med. Chem.* 46 (14) 2813–2815.

Lee, C. T., Yang, W. T., Parr, R. G. (1988). Development of the colle-salvetti correlation-energy formula into a functional of the electron density. *Physical Review B*, 37, 785-789

Liu, M., Wilairat, P., Go, M.L. (2001). Antimalarial alkoxylated and hydroxylated chalcones: Structure-activity relationship analysis. *J Med Chem*. 44 (25): 4443-4452.

Middleton, E.; Kandaswami, C.; Theoharides, T. C. (2000) The effects of plant flavonoids on mammalian cells: Implications for inflammation, heart disease, and cancer. *Pharmacol. Rev*., 52, 673-751.

Nowakowska, Z., A review of anti-infective and anti-inflammatory chalcones. *Eur. J. Med. Chem*. 2007, 42, 125-137.

Ravichandran, R., Rajendran, M., Devapiriam, D.(2013). Studies on chalcone derivatives antioxidant and stability constant. *J Chem Bio Phy Sci Sec A*. 3 (4): 2446-2458.

Reddy, L.S.S., Raju, M.B. and Sridhar, C. (2016). Novel Pyrazolınes: Synthesıs and Evaluatıon of Theır Derıvatıves wıth Antıcancer and Antı-Inflammatory Actıvıtıes. *Int J Pharm Pharm Sci.* 8, 247.

Saxena, H.O., Faridi, U., Kumar, J.K., Luqman, S., Darokar, M.P., Shanker, K., Chanotiya, C.S., Gupta, M.M., Negi, A.S. (2007) Synthesis of chalcone derivatives on steroidal framework and their anticancer activities, *Steroids*. 72 (13) 892–900.

Shakil, N.A., Singh, M.K., Sathiyendiran, M., Kumar, J., Padaria, J.C. (2013) Microwave synthesis, characterization and bio-efficacy evaluation of novel chalcone based 6-carbethoxy-2-cyclohexen-1-one and 2H-indazol-3-ol derivatives. *Eur. J. Med. Chem*. 120–31.

Tanaka, H., Nakamura, S., Onda, K., Tazaki, T., Hirano, T. (2009). Sofalcone, an anti-ulcer chalcone derivative, suppresses inflammatory crosstalk between macrophages and adipocytes and adipocyte differentiation: implication of heme-oxygenase-1 induction. Biochem Biophys Res Commun 381: 566-571.

Ugurlu, G., Kasap, E., Kantarci, Z., Bahat, M. (2007), A theoretical study of the linear, nonlinear optical properties and conformational analysis of 3-phenylthiophene and its fluoro derivatives with torsional dependence. *Journal of Molecular Structure*. 834–836, 508–515.

Uğurlu, G., Beytur, M. (2020) Theoretical studies on the structural, vibrational, conformational analysis and nonlinear optic property of 4-(methoxycarbonyl)-phenylboronic acid. *Indian Journal of Chemistry*. Vol. 59A, pp. 1504-1512.

Uğurlu, G., NECEFOĞLU. H. (2018) Theoretical investigation on the structural and electronic properties of (1-naphthylmethylidene)isonicotinohydrazide molecule. *Iğdır Univ. J. Inst. Sci. & Tech*. 8(2): pp.167-177.

Uğurlu, G. (2020)Theoretical examination of the conformational effect on the molecular structure and electronic properties of the orthorhombic metaboric acid molecule. BORON 5 (2), pp. 91 – 99.

Vazquez-Vuelvas, O.F., Enriquez-Figueroa, R.´ A., Garcia-Ortega, H., Flores-Alamo, M., Pineda-Contreras, A. (2015). Crystal structure of the chalcone (E)-3-(furan-2-yl)- 1-phenylprop-2-en-1-one. *Acta Cryst.* E71, 161–164.